

Solution of Diffusion Equations Involved in Drying Fruit Slice using Reduced Differential Transform Method

Saroj R. Yadav and Parth T. Parmar

Abstract—Drying is a complicated process that requires the simultaneous transfer of heat and mass. Mathematical modeling of the drying process in agro-products is important to encapsulate the original flavor and maintain nutritional value in dried food product. Models involving PDEs are solved that can be used to maintain the moisture and temperature within a fruit slice by drying it. A new initiative is to produce dried fruit product due to increasing demand of dry fruits for easy storage. The aim of this work is to solve diffusion equations involving moisture and temperature that can be used to maintain the moisture and temperature within a fruit slice by drying it. The results are obtained analytically by solving the diffusion equations in 1D, 2D and 3D using the reduced differential transform method. The results are then analyzed by changing the input parameters, such as moisture diffusivity and thermal diffusivity. Graphical plots of moisture and temperature distribution are analyzed for agreement between the results obtained and published numerical and experimental results.

Index Terms—diffusion; moisture and temperature; drying fruit slice; mathematical model; reduced differential transform method.

I. INTRODUCTION

THE process of removing water or other liquids from a solution, suspension, or other solid-liquid mixture to generate a dry solid is known as drying. It is a challenging procedure that requires the simultaneous transmission of heat and mass. Fruits have intricate and diverse biological structures making it necessary to use unique drying models for each fruit type to maintain quality. This poses inherent challenges, which is where modeling and simulation techniques prove valuable. The standard approach involves creating a mathematical model based on heat and mass transfer principles. This model accounts for assumptions related to mass transfer parameters including material properties, transport equations, initial and boundary conditions and the analytical or numerical solution of partial differential equations (PDEs). These models are then applied for the computational simulation of the drying process. Direct (convection), indirect or contact (conduction), radiant (radiation) and dielectric or microwave (radio frequency) drying are the four types of drying. Throughout the years, much research has been conducted on the drying of fruits such as apples, grapes, berries, bananas, pears and so on.

Sherwood and Lewis are widely considered the founders of drying models in mathematics. In 1920, Lewis proposed the theory of liquid diffusion on the basis of migration

of moisture content in the form of liquid diffusion during drying of solid materials. The driving force of this migration was the internal moisture content gradient [1]. Sherwood proposed theory of drying diffusion in solid material similar to theory of Lewis in 1929[1]. Since then many papers are published on experimental and mathematical study of drying of various fruits and vegetables. Many mathematical models are proposed considering various aspects like models involving empirical relations valid under specific conditions, models given on heat and moisture diffusion giving system of simultaneous PDEs, few models considered energy, mass and momentum transport equations[2], [3]. Lemuel N. Diamante et al.[4] developed a model for drying fruits with a thin layer. Many researchers has done experimental studies to mathematically model drying of various fruit slices. They tested two types of fruits, kiwifruit and apricot at three different temperatures (60 °C, 80 °C, 100 °C). Irci Turk Toglun and Dursun Pehlivan [5] conducted an open-air drying experiment to examine the behavior of fruits apricots pre-sulphured with SO₂ or NaHSO₃, grapes, peaches, figs, and plums while drying under natural conditions. Multiple regression analysis was used to investigate the impact of the surface temperature of the fruits and the relative humidity just above their surface on the constants and coefficients of the chosen models. Shahpouri Jahedi Rad et al. [6] studied the white mulberry, which was experimentally dried out under thin layer convective-infrared conditions at infrared power levels of 500W, 1000W, and 1500W, drying air temperatures of 40 °C, 55 °C, and 70 °C, and input drying air velocity of 0.4, 1 and 1.6 m s⁻¹. J.A Esfahani et al.[7] considered moist slab cut pieces of apple with the length of 8 centimeter, L = 8 cm and height of 2 centimeter, H = 2 cm, analyzed the external flow and temperature with three different inlet velocities. They obtained the average convective heat and mass transfer coefficients and solved 2D heat and mass transfer equations using the separation of variables method in the form of a multiple of two separated one-dimensional solution. They also validated the analytical solution with the numerical drying data.

A.M. Castro et al.[8] have given detailed review on mathematical modelling of convective drying of fruit. They have listed representative macroscale mathematical models (heat transport equations, mass transport equations and momentum equations) and microscale mathematical models (heat transfer equations, mass transfer equations, air equations for conjugated models and equations for hybrid technologies) of transport phenomena during convective drying of fruit considered by researchers. Many numerical and analytical techniques can be utilized to solve the complicated partial differential equations of coupled heat, mass, and momentum

Manuscript received August 4, 2023; revised February 29, 2024

Saroj R. Yadav is an assistant professor in the Department of Mathematics, SVNIT, Surat, Gujarat, India (e-mail: sry@amhd.svnit.ac.in)

Parth Parmar is a researcher in the Department of Mathematics, SVNIT, Surat, Gujarat, India (e-mail: parthparmar3431@gmail.com)

transport that must be solved for the modeling [8]. In this review A.M. Castro et al.[8] have also included various numerical and analytical methods used by researchers to solve governing PDEs.

In the present study, the coupled PDE of the diffusion equations is considered which provides the physical equations that regulate the simultaneous transmission of moisture $M(t)$ and temperature $T(t)$ in an isotropic fruit without internal moisture sources [3], [9]. In this model, the coupled PDE of the diffusion equations has been solved by the Reduced Differential Transform Method(RDTM).The coupled PDEs of the diffusion equations are considered as;

$$\frac{\partial M}{\partial t} = \nabla \cdot (D\nabla M), \tag{1}$$

$$\rho c_p \frac{\partial T}{\partial t} = \nabla \cdot (\kappa \nabla T). \tag{2}$$

The diffusion coefficient, density, specific heat capacity, and thermal conductivity are taken as D , ρ , c_p , and κ , respectively. The temperature in the example above is calculated using a common heat conduction formulation, and the conductive temperature flux is $q = -\kappa \nabla T$. Equation(1) represents the movement of moisture inside the slice during drying, while equation(2) reflects the evolution of temperature inside the slice.

II. CALCULATION METHOD

The ‘Differential Transform Method’ (DTM) is a semi-analytical technique for generating analytical and numerical solutions to a wide variety of differential equations. The differential transform was first proposed by Zhou [10], and it is primarily used in circuit analysis to solve both linear as well as nonlinear IVPs. This approach yields an analytical solution based on polynomials. It differs from the usual Taylor series approach, which requires a symbolic calculation of the required output of another data function. Taylor’s technique is highly time-consuming for larger orders. Similar to a Taylor series of several mathematical equations, DTM creates a sequence of iterations.

This method constructs an analytical solution in the form of a polynomial and uses it as the approximation to exact solutions which are sufficiently differentiable [11], [12], [13], [14]. Moreover, This method neither requires any condition for the convergence of solution nor does rely on grids or mesh. This can be advantageous when dealing with irregular domains or when traditional grid-based methods are challenging to apply. Later on, this method was modified to a new method called reduced differential transform method(RDTM) and this method became more popular as it improved the speed of computation.

A. Reduced differential transform method

The RDTM was first proposed by the Turkish mathematician Keskin [[15],[16],[17]] in 2009. It has received much attention since it has been applied to solve a wide variety of problems by many authors[18]. In RDTM, the differentiation is taken with respect to time variable only.

Assume that a function of two variables $u(x, t)$, can be written as the product of two functions $u(x, t) = f(x)g(t)$.

The function $u(x, t)$ may be expressed as follow based on the characteristics of the one-dimensional differential transform:

$$u(x, t) = \left(\sum_{i=0}^{\infty} F(i)x^i \right) \left(\sum_{j=0}^{\infty} G(j)t^j \right) = \sum_{k=0}^{\infty} U_k(x)t^k,$$

The t -dimensional spectrum of function $u(x, t)$ is termed as $U_k(x)$. The basic definitions of RDTM have been discussed in [[15],[16],[17]] as given below.

Definition 1. Let $u(x, t)$ be an analytic and continuously differentiable function with respect to time t and space x in the domain of interest, then

$$U_k(x) = \frac{1}{k!} \left[\frac{\partial^k}{\partial x^k} u(x, t) \right]_{t=0},$$

where the t -dimensional spectrum function $U_k(x)$ is the transformed function. In this study, the original function is denoted by the lowercase letter $u(x, t)$, while the transformed function is denoted by the uppercase letter $U_k(x)$.

Definition 2. The following definition applies to the differential inverse transform of $U_k(x)$:

$$u(x, t) = \sum_{k=0}^{\infty} U_k(x)t^k.$$

When we combine both equations, we get the result

$$u(x, t) = \sum_{k=0}^{\infty} \frac{1}{k!} \left[\frac{\partial^k}{\partial x^k} u(x, t) \right]_{t=0} t^k.$$

The basic mathematical operations of one-dimensional differential transform are given in Table (I).

Table I: Fundamental operation of RDTM w.r.t variable t

Original function	Transformed function
$u_1(x, t) \pm u_2(x, t)$	$U_1(x) \pm U_2(x)$
$\lambda u_1(x, t)$	$\lambda U_1(x)$
$\frac{\partial}{\partial x} u(x, t)$	$\frac{\partial}{\partial x} U_k(x)$
$\frac{\partial^r}{\partial t^r} u(x, t)$	$\frac{(k+r)!}{k!} U_{k+r}(x)$
$u(x, t) \cdot v(x, t)$	$\sum_{r=0}^k U_r(x) V_{k-r}(x)$
$x^a t^b$	$x^a \delta(h-b)$ where $\delta(h-b) = \begin{cases} 1, & h = b \\ 0, & h \neq b \end{cases}$

Theorem 1. If $z(x, t) = \frac{\partial^m}{\partial x^m} u(x, t)$, then $Z_k(x) = \frac{\partial^m}{\partial x^m} U_k(x)$.

Theorem 2. If $z(x, t) = \frac{\partial^m}{\partial t^m} u(x, t)$, then $Z_k(x) = \frac{(k+m)!}{k!} U_{k+m}(x)$.

B. Implementation of RDTM

To illustrate the implementation of RDTM to solve non-linear pde, let’s consider the non-linear PDE:

$$\frac{\partial^r}{\partial t^r} w(x, t) + Lw(x, t) + Nw(x, t) = h(x, t), \quad t > 0, \tag{3}$$

with initial conditions

$$w^{(k)}(x, 0) = g_k(x), k = 0, 1, \dots, (r - 1), \quad (4)$$

where $r \in \mathbb{N}$, L is a linear operator, N is a non linear operator and $h(x, t)$ is in inhomogeneous term.

The fundamental operation of RDTM from Table 1 converts Eqs (3) and (4) to recursive formula given by:

$$\frac{(k+r)!}{k!} W_{k+r}(x) + L W_k(x) + N W_k(x) = H_k(x), \quad (5)$$

and the transformed initial condition is

$$W^{(k)}(x) = G_k(x), k = 0, 1, 2, \dots, (r - 1), \quad (6)$$

where $W_k(x)$ and $H_k(x)$ are transformed form of the original function $w(x, t)$ and $h(x, t)$ obtained by applying RDTM in the k^{th} iteration. Substituting the value of $W_{k+r}(x)$ for $k = 0, 1, 2, \dots, (r - 1)$ in definition of inverse reduced differential transform, the approximate analytical series solution of (3) with initial condition (4) is given by

$$w(x, t) = \sum_{k=0}^{\infty} W_k(x) t^k. \quad (7)$$

C. Convergence and error analysis of RDTM

RDTM gives the approximate analytical series solution (7) of the non-linear pde given in (3), the principal aim of this section is to discuss the sufficient conditions for convergence of this solution. For this purpose, some theorems for convergence of the method and the error computation are addressed in [21]. To get the solution of the considered problem includes ascertaining power series expansion in (7) with the initial time $t = 0$:

$$w(x, t) = \sum_{k=0}^{\infty} a_k(x) t^k, \quad t \in l, \quad (8)$$

where $l = (0, r), r > 0$. The important results on convergence and error estimation are given in the theorems below [21].

Theorem 3. If $\phi_k(x, t) = a_k(x) t^k$, then the series solution $\sum_{k=0}^{\infty} a_k(x) t^k$, stated in (8), $\forall k \in \mathbb{N} \cup \{0\}$.

(i) It is convergent if $\exists 0 < \lambda < 1$ such that $\|\phi_{k+1}\| \leq \lambda \|\phi_k\|$.

(ii) It is divergent if $\lambda > 1$ such that $\|\phi_{k+1}\| \geq \lambda \|\phi_k\|$.

Theorem 4. Suppose that the series solution $\sum_{k=0}^{\infty} \phi_k(x, t)$, where $\phi_k(x, t) = a_k(x) t^k$, converges to the solution $w(x, t)$. If the truncated series $\sum_{k=0}^m \phi_k(x, t)$ is used as an approximation to the solution $u(x, t)$, then the maximum absolute truncated error is estimated as

$$\left\| w(x, t) - \sum_{k=0}^m \phi_k(x, t) \right\| \leq \frac{1}{1-\lambda} \lambda^{m+1} \|\phi_0\| \quad (9)$$

III. MATHEMATICAL MODELS

In this section mathematical models for simultaneous transmission of heat and moisture in drying fruit slice are considered for 1D, 2D and 3D cases. Moisture content and temperature profile inside the fruit slice are obtained for all three cases from solution of governing pdes by RDTM.

A. One Dimensional fruit drying model

In this part, we use the general heat and mass transfer formulation to create a simple model of moisture and heat distribution during fruit drying. The physical model comprises of a single slice of fruit having thickness $2L$, with non-uniform initial temperature $T_0 - T_1 \cos\left(\frac{\pi x}{2L}\right)$ and moisture content $M_0(1 + \cos\left(\frac{\pi x}{2L}\right))$. As shown in figure (1), $x = 0$ is the mid-plane of the fruit slice and drying is assumed to be effective only at out surfaces $x = \pm L$.

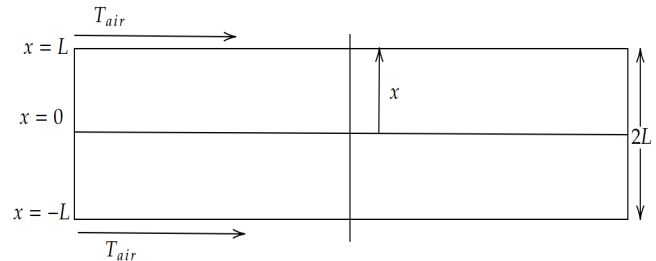


Figure 1: Schematic diagram of 1D model of drying fruit slice

As illustrated in figure (1), the problem under consideration is symmetric about the midplane $x = 0$ of the fruit slice.

At the time of the drying process, most of the heat is carried through convection from the air to the fruit slice's outside surface, then by conduction to the inside. Evaporation is the process by which moisture is released into the atmosphere as it moves towards the surface. A model for the simultaneous transmission of heat and moisture is developed to explain such a coordinated process [19],

$$\rho_s \frac{\partial M}{\partial t} = \frac{\partial}{\partial x} \left(D \rho_s \frac{\partial M}{\partial x} \right); \quad 0 < x < L_x, \quad (10)$$

$$\rho_s C_p \frac{\partial T}{\partial t} = \frac{\partial}{\partial x} \left(\kappa \frac{\partial T}{\partial x} \right); \quad 0 < x < L_x. \quad (11)$$

The coefficient of diffusion, density of the solid, specific heat capacity, and thermal conductivity are denoted by D , ρ_s , C_p , and κ respectively. For this 1D model, we are considering the outer surfaces at $L = L_x$ for variable x . Due to symmetry, the solution is examined from $x = 0$ to $x = L_x$. For constant thermal diffusivity $\alpha_0 = \frac{\kappa}{\rho_s C_p}$ and constant diffusion coefficient $D = D_0$ equation (10) and (11) results into;

$$\frac{\partial M}{\partial t} = D_0 \frac{\partial^2 M}{\partial x^2}; \quad 0 < x < L_x, \quad (12)$$

$$\frac{\partial T}{\partial t} = \alpha_0 \frac{\partial^2 T}{\partial x^2}; \quad 0 < x < L_x. \quad (13)$$

Both, the amount of moisture present and the temperature are considered to be non-uniform throughout the drying process, whereas neglecting the shrinkage effect the thickness of the slice is taken as uniform. At $t = 0$ non-uniform distribution of moisture content and the temperature profile is considered as initial conditions taken in (14);

$$\begin{aligned} M(x, 0) &= M_0 \left[1 + \cos\left(\frac{\pi x}{2L_x}\right) \right], \\ T(x, 0) &= T_0 - T_1 \cos\left(\frac{\pi x}{2L_x}\right). \end{aligned} \quad (14)$$

The center of the slice at $x = 0$ has no temperature or moisture gradients; hence, the following conditions hold [19];

$$\frac{\partial M}{\partial x} = 0, \quad \frac{\partial T}{\partial x} = 0 \text{ at } x = 0. \quad (15)$$

At the surface boundary, heat transmission is caused by convection to the dry air above, and this phenomenon is often represented by a heat transfer coefficient h . The surface boundary condition is determined by the amount of heat that is absorbed by moisture when it changes from the liquid to the gaseous phase [19],

$$\kappa \frac{\partial M}{\partial x} - \lambda D_0 \rho_s \frac{\partial T}{\partial x} = -h(T_{sur} - T_{air}) \text{ at } x = L_x, \quad (16)$$

where λ is the latent heat.

When establishing a drying surface boundary condition, we must consider a driving gradient. Temperature and pressure make up this gradient. The difference between C_{air} and C_{sur} is what makes water vapor move from a wet surface into the air [19], therefore

$$-D_0 \rho_s \frac{\partial M}{\partial x} = h_m(C_{sur} - C_{air}) \text{ at } x = L_x. \quad (17)$$

The above (12) and (13) along with the initial condition (14) and boundary conditions (15), (16) and (17) gives partial differential equation model to describe the moisture distribution and temperature distribution in the fruit slices.

Applying reduced differential transform on (12) and (13), we get

$$\frac{(k+1)!}{k!} M_{k+1}^*(x) = D_0 \frac{\partial^2}{\partial x^2} M_k^*(x), \quad (18)$$

$$\frac{(k+1)!}{k!} T_{k+1}^*(x) = \alpha_0 \frac{\partial^2}{\partial x^2} T_k^*(x), \quad (19)$$

where M_i^* and T_i^* are the transformed functions, $i \in \mathbb{Z}^+$. On applying the transformation to the initial conditions (14), we have

$$\begin{aligned} M_0^*(x) &= M_0 \left[1 + \cos\left(\frac{\pi x}{2L_x}\right) \right], \\ T_0^*(x) &= T_0 - T_1 \cos\left(\frac{\pi x}{2L_x}\right). \end{aligned} \quad (20)$$

On using (20) in (18), we get

$$\begin{aligned} \frac{1!}{0!} M_1^*(x) &= D_0 \frac{\partial^2}{\partial x^2} M_0^*(x) \\ &= D_0 \frac{\partial^2}{\partial x^2} \left[M_0 \left\{ 1 + \cos\left(\frac{\pi x}{2L_x}\right) \right\} \right] \\ &= -D_0 M_0 \left(\frac{\pi}{2L}\right)^2 \cos\left(\frac{\pi x}{2L_x}\right). \end{aligned}$$

Similarly, on taking $k = 1$, we get

$$\begin{aligned} \frac{2!}{1!} M_2^*(x) &= D_0 \frac{\partial^2}{\partial x^2} M_1^*(x) \\ M_2^*(x) &= \frac{1}{2} D_0 \frac{\partial^2}{\partial x^2} \left[-D_0 M_0 \left(\frac{\pi}{2L_x}\right)^2 \cos\left(\frac{\pi x}{2L_x}\right) \right] \\ &= \frac{1}{2} D_0^2 M_0 \left(\frac{\pi}{2L_x}\right)^4 \cos\left(\frac{\pi x}{2L_x}\right). \end{aligned}$$

Thus, the general term can be defined as

$$M_k^*(x) = \frac{M_0}{k!} \left[\left(-D_0 \frac{\pi^2}{4L_x^2} \right)^k \cos\left(\frac{\pi x}{2L_x}\right) \right]; \quad k > 0.$$

Using the reverse transformation on $M_k^*(x)$, we get

$$\begin{aligned} M(x, t) &= \sum_{k=0}^{\infty} M_k^*(x) t^k \\ &= M_0 \left[1 + \sum_{k=0}^{\infty} \frac{1}{k!} \left(\frac{-D_0 \pi^2 t}{4L_x^2} \right)^k \cos\left(\frac{\pi x}{2L_x}\right) \right] \\ &= M_0 \left[1 + \exp\left\{ \left(\frac{-D_0 t \pi^2}{4L_x^2} \right) \right\} \cos\left(\frac{\pi x}{2L_x}\right) \right]. \end{aligned} \quad (21)$$

The above (21) shows the moisture content for the fruit slice for any layer in $0 < x < L_x$ at any time t .

Now, we will solve (13) to obtain the temperature inside the fruit slice for any layer at any time t .

So, we substitute (20) in (19) at $k = 0$ to get

$$\begin{aligned} \frac{1!}{0!} T_1^*(x) &= \alpha_0 \frac{\partial^2}{\partial x^2} T_0^*(x) \\ &= \alpha_0 \frac{\partial^2}{\partial x^2} \left[T_0 - T_1 \cos\left(\frac{\pi x}{2L_x}\right) \right] \\ &= -\alpha_0 T_1 \left(\frac{\pi}{2L_x}\right)^2 \cos\left(\frac{\pi x}{2L_x}\right). \end{aligned}$$

Similarly,

$$\begin{aligned} \frac{2!}{1!} T_2^*(x) &= \alpha_0 \frac{\partial^2}{\partial x^2} T_1^*(x) \\ T_2^*(x) &= \frac{1}{2} \alpha_0 \frac{\partial^2}{\partial x^2} \left[-\alpha_0 T_1 \left(\frac{\pi}{2L_x}\right)^2 \cos\left(\frac{\pi x}{2L_x}\right) \right] \\ &= \frac{1}{2} \alpha_0^2 T_1 \left(\frac{\pi^2}{4L_x^2}\right)^2 \cos\left(\frac{\pi x}{2L_x}\right). \end{aligned}$$

Thus, the general term can be defined as

$$T_k^*(x) = \frac{T_1}{k!} \left(\frac{-\alpha_0 \pi^2}{4L_x^2} \right)^k \cos\left(\frac{\pi x}{2L_x}\right); \quad k > 0.$$

Using the inverse transformation on $T_k^*(x)$, we get the temperature $T(x, t)$ in the fruit slice as;

$$\begin{aligned} T(x, t) &= \sum_{k=0}^{\infty} T_k^*(x) t^k \\ &= T_0 - T_1 \sum_{k=0}^{\infty} \frac{1}{k!} \left(\frac{-\alpha_0 t \pi^2}{4L^2} \right)^k \cos\left(\frac{\pi x}{2L}\right) \\ &= T_0 - T_1 \exp\left\{ \left(\frac{-\alpha_0 \pi^2 t}{4L^2} \right) \right\} \cos\left(\frac{\pi x}{2L}\right). \end{aligned} \quad (22)$$

Eq. (21) and (22) are the solutions to the diffusion equations describing moisture content and temperature content in the fruit slice.

B. Two Dimensional fruit drying slice

In the two-dimensional model, we suppose that there is a fruit slice of infinite length, and the moisture and temperature are spread unevenly over the thickness and width of the fruit. We are now considering the possibility of drying a piece of fruit slice in the form of a rectangle: $x = \pm L_x$, $y = \pm L_y$. The initial moisture and temperature content of the

fruit slice are assumed to be non-uniform such that moisture in the centre is maximum and temperature on outer surface is maximum. So, the initial moisture content and temperature content are taken as;

$$M(x, y, 0) = M_0 \left\{ 1 + \cos \left(\frac{\pi x}{2L_x} \right) \cdot \cos \left(\frac{\pi y}{2L_y} \right) \right\}, \quad (23)$$

and

$$T(x, y, 0) = T_0 - T_1 \left\{ \cos \left(\frac{\pi x}{2L_x} \right) \cdot \cos \left(\frac{\pi y}{2L_y} \right) \right\}, \quad (24)$$

From diffusion equations (1) and (2), generalising pde model from (10) and (11), we have 2-dimensional model to describe simultaneous transmission of heat and moisture in the fruit slice as (25) and (26);

$$\rho_s \frac{\partial M}{\partial t} = \frac{\partial}{\partial x} \left(D \rho_s \frac{\partial M}{\partial x} \right) + \frac{\partial}{\partial y} \left(D \rho_s \frac{\partial M}{\partial y} \right); \quad (25)$$

$$0 < x < L_x, \quad 0 < y < L_y,$$

$$\rho_s C_p \frac{\partial T}{\partial t} = \frac{\partial}{\partial x} \left(k \frac{\partial T}{\partial x} \right) + \frac{\partial}{\partial y} \left(k \frac{\partial T}{\partial y} \right); \quad (26)$$

$$0 < x < L_x, \quad 0 < y < L_y.$$

The coefficient of diffusion, density of the solid, specific heat capacity, and thermal conductivity are denoted by D , ρ_s , C_p and κ respectively. Due to symmetry, the solution is examined from $x = 0$ to $x = L_x$ and $y = 0$ to $y = L_y$. Thermal diffusivity $\alpha_0 = \frac{\kappa}{\rho_s C_p}$ and diffusion coefficient $D = D_0$ are taken as constants. Hence,

$$\frac{\partial M}{\partial t} = D_0 \left(\frac{\partial^2 M}{\partial x^2} + \frac{\partial^2 M}{\partial y^2} \right); \quad (27)$$

$$0 < x < L_x, \quad 0 < y < L_y$$

$$\frac{\partial T}{\partial t} = \alpha_0 \left(\frac{\partial^2 T}{\partial x^2} + \frac{\partial^2 T}{\partial y^2} \right); \quad (28)$$

$$0 < x < L_x, \quad 0 < y < L_y$$

with initial condition from (23) and (24) as

$$M(x, y, 0) = M_0 \{ 1 + \cos px \cdot \cos qy \}, \quad (29)$$

$$T(x, y, 0) = T_0 - T_1 \{ \cos px \cdot \cos qy \}, \quad (30)$$

where $p = \frac{\pi}{2L_x}$ and $q = \frac{\pi}{2L_y}$.

Assuming symmetry, there are no temperature gradients or moisture concentration gradients at the center of slice, and as a result the following conditions hold [19];

$$\frac{\partial M}{\partial x} = 0 \ \& \ \frac{\partial T}{\partial x} = 0, \text{ at } x = 0 \quad (31)$$

$$\frac{\partial M}{\partial y} = 0 \ \& \ \frac{\partial T}{\partial y} = 0, \text{ at } y = 0 \quad (32)$$

At the surface, boundary conditions become[19];

$$\begin{aligned} \kappa \frac{\partial M}{\partial x} - \lambda D_0 \rho_s \frac{\partial T}{\partial x} &= -h(T_{sur} - T_{air}) \\ -D_0 \rho_s \frac{\partial M}{\partial x} &= h_m(C_{sur} - C_{air}) \text{ at } x = L_x \end{aligned} \quad (33)$$

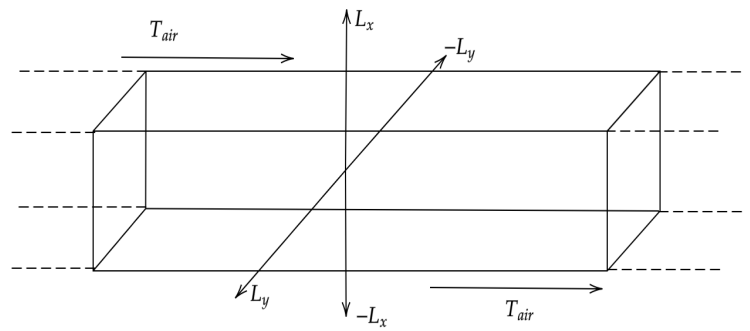


Figure 2: Schematic diagram of 2D model of drying fruit slice process

$$\begin{aligned} \kappa \frac{\partial M}{\partial y} - \lambda D_0 \rho_s \frac{\partial T}{\partial y} &= -h(T_{sur} - T_{air}) \\ -D_0 \rho_s \frac{\partial M}{\partial y} &= h_m(C_{sur} - C_{air}) \text{ at } y = L_y \end{aligned} \quad (34)$$

figure(2) illustrates a two-dimensional isotropic fruit slice for symmetric drying circumstances.

Now, we will use the RDTM to derive moisture and temperature in the fruit slice from (27) and (28), applying RDTM we have;

$$\frac{(k+1)!}{k!} M_{k+1}^*(x, y) = D_0 \left\{ \frac{\partial^2}{\partial x^2} + \frac{\partial^2}{\partial y^2} \right\} M_k^*(x, y), \quad (35)$$

$$\frac{(k+1)!}{k!} T_{k+1}^*(x, y) = \alpha_0 \left\{ \frac{\partial^2}{\partial x^2} + \frac{\partial^2}{\partial y^2} \right\} T_k^*(x, y). \quad (36)$$

On applying RDTM on the initial condition (29) and (30) we get

$$M_0^*(x, y) = M_0 \{ 1 + \cos px \cdot \cos qy \}, \quad (37)$$

$$T_0^*(x, y) = T_0 - T_1 \{ \cos px \cdot \cos qy \}. \quad (38)$$

By taking $k = 0$ and substituting (37) in (35) and (38) in (36), we obtain

$$\begin{aligned} \frac{1!}{0!} M_1^*(x, y) &= D_0 \left\{ \frac{\partial^2}{\partial x^2} M_0^*(x, y) + \frac{\partial^2}{\partial y^2} M_0^*(x, y) \right\} \\ &= M_0 (-D_0) \cos px \cdot \cos qy \{ p^2 + q^2 \}. \end{aligned} \quad (39)$$

$$\begin{aligned} \frac{1!}{0!} T_1^*(x, y) &= \alpha_0 \left\{ \frac{\partial^2}{\partial x^2} T_0^*(x, y) + \frac{\partial^2}{\partial y^2} T_0^*(x, y) \right\} \\ &= T_1 \cdot \alpha_0 \cdot \cos px \cdot \cos qy \{ p^2 + q^2 \}. \end{aligned} \quad (40)$$

By taking $k = 1$ and substituting (39) in (35) and (40) in (36), we obtain

$$\begin{aligned} \frac{2!}{1!} M_2^*(x, y) &= D_0 \left\{ \frac{\partial^2}{\partial x^2} M_1^*(x, y) + \frac{\partial^2}{\partial y^2} M_1^*(x, y) \right\}, \\ M_2^*(x, y) &= \frac{1}{2} M_0 D_0^2 \cos px \cdot \cos qy \{ p^2 + q^2 \}^2. \end{aligned} \quad (41)$$

$$\begin{aligned} \frac{2!}{1!} T_2^*(x, y) &= \alpha_0 \left\{ \frac{\partial^2}{\partial x^2} T_1^*(x, y) + \frac{\partial^2}{\partial y^2} T_1^*(x, y) \right\}, \\ T_2^*(x, y) &= \frac{-1}{2} T_1 \cdot \alpha_0^2 \cdot \cos px \cdot \cos qy \{ p^2 + q^2 \}^2. \end{aligned} \quad (42)$$

By taking $k = 2$ and substituting (39) in (35), we obtain

$$\frac{3!}{2!} M_3^*(x, y) = D_0 \left\{ \frac{\partial^2}{\partial x^2} M_2^*(x, y) + \frac{\partial^2}{\partial y^2} M_2^*(x, y) \right\},$$

$$M_3^*(x, y) = \frac{1}{6} M_0 (-D_0)^3 \cos px \cdot \cos qy \{p^2 + q^2\}^3. \quad (43)$$

$$\frac{3!}{2!} T_3^*(x, y) = \alpha_0 \left\{ \frac{\partial^2}{\partial x^2} T_2^*(x, y) + \frac{\partial^2}{\partial y^2} T_2^*(x, y) \right\}, \quad (44)$$

$$T_3^*(x, y) = \frac{1}{6} T_1 \cdot \alpha_0^3 \cdot \cos px \cdot \cos qy \{p^2 + q^2\}^3.$$

Thus, using (37), (38), (39), (40), (41), (42) & (43), we get

$$M_k^*(x, y) = M_0 \frac{-D_0^k}{k!} \cos px \cdot \cos qy \{p^2 + q^2\}^k, \quad (45)$$

$$T_k^*(x, y) = -T_1 \cdot \frac{(-\alpha_0)^k}{k!} \cdot \cos px \cdot \cos qy \{p^2 + q^2\}^k, \quad (46)$$

where $k \in \mathbb{N}$

using inverse transformation of $M_k^*(x, y)$ and $T_k^*(x, y)$ yields

$$M(x, y, t) = \sum_{k=0}^{\infty} M_k^*(x, y) t^k$$

$$= M_0^*(x, y) + \sum_{k=1}^{\infty} M_k^*(x, y) t^k$$

$$= M_0 \{1 + \cos px \cdot \cos qy\}$$

$$+ M_0 \cos px \cdot \cos qy \sum_{k=1}^{\infty} \frac{-D_0^k}{k!} \{p^2 + q^2\}^k t^k.$$

$$M(x, y, t) = M_0 \left[1 + \cos px \cdot \cos qy \cdot e^{-D_0(p^2+q^2)t} \right]. \quad (47)$$

and

$$T(x, y, t) = \sum_{k=0}^{\infty} T_k^*(x, y) t^k$$

$$= T_0^*(x, y) + \sum_{k=1}^{\infty} T_k^*(x, y) t^k$$

$$= T_0 - T_1 \cdot \cos px \cdot \cos qy$$

$$- \sum_{k=1}^{\infty} T_1 \cdot \frac{(-\alpha_0)^k}{k!} \cdot \cos px \cdot \cos qy \{p^2 + q^2\}^k t^k.$$

$$T(x, y, t) = T_0 - T_1 \cos px \cdot \cos qy \cdot e^{-\alpha_0(p^2+q^2)t}. \quad (48)$$

C. Three Dimensional fruit drying slice

In our three-dimensional model, we introduce the concept of finite dimensions for the fruit slice, considering its length, width and height. This expansion allows us to account for uneven distribution of both moisture and temperature across the thickness, height and width of the fruit. We now look into drying a portion of fruit slice that takes the shape of a cuboid, defined by its boundaries as $x = \pm L_x$, $y = \pm L_y$, and $z = \pm L_z$.

The initial moisture and temperature content of the fruit slice are considered to be as follows:

$$M(x, y, z, 0) = M_0 \{1 + \cos px \cdot \cos qy \cdot \cos rz\} \quad (49)$$

and

$$T(x, y, z, 0) = T_0 - T_1 \{\cos px \cdot \cos qy \cdot \cos rz\}, \quad (50)$$

where $p = \frac{\pi}{2L_x}$, $q = \frac{\pi}{2L_y}$ and $r = \frac{\pi}{2L_z}$.

Considering diffusion equations (49) and (50) in 3-dimensions as;

$$\frac{\partial M}{\partial t} = \frac{\partial}{\partial x} \left(D_0 \frac{\partial M}{\partial x} \right) + \frac{\partial}{\partial y} \left(D_0 \frac{\partial M}{\partial y} \right) + \frac{\partial}{\partial z} \left(D_0 \frac{\partial M}{\partial z} \right);$$

$$0 < x < L_x, 0 < y < L_y, 0 < z < L_z, \quad (51)$$

$$\rho_s C_p \frac{\partial T}{\partial t} = \frac{\partial}{\partial x} \left(\kappa \frac{\partial T}{\partial x} \right) + \frac{\partial}{\partial y} \left(\kappa \frac{\partial T}{\partial y} \right) + \frac{\partial}{\partial z} \left(\kappa \frac{\partial T}{\partial z} \right);$$

$$0 < x < L_x, 0 < y < L_y, 0 < z < L_z. \quad (52)$$

The coefficient of diffusion is represented as D_0 , the density of solid as ρ_s , the specific heat capacity as C_p , and the thermal conductivity as κ . To maintain simplicity, we examine the solution within range from $x = 0$ to $x = L_x$, $y = 0$ to $y = L_y$ and $z = 0$ to $z = L_z$ due to the inherent symmetry of the problem.

Additionally, considering two fundamental constants: thermal diffusivity, denoted as α_0 and calculated as $\frac{\kappa}{\rho_s C_p}$, and the diffusion coefficient, marked as D and kept at a constant value of D_0 . (44) and (45) yield

$$\frac{\partial M}{\partial t} = D_0 \left(\frac{\partial^2 M}{\partial x^2} + \frac{\partial^2 M}{\partial y^2} + \frac{\partial^2 M}{\partial z^2} \right);$$

$$0 < x < L_x, 0 < y < L_y, 0 < z < L_z, \quad (53)$$

$$\frac{\partial T}{\partial t} = \alpha_0 \left(\frac{\partial^2 T}{\partial x^2} + \frac{\partial^2 T}{\partial y^2} + \frac{\partial^2 T}{\partial z^2} \right);$$

$$0 < x < L_x, 0 < y < L_y, 0 < z < L_z. \quad (54)$$

figure(3) illustrates a three-dimensional isotropic fruit slice for symmetric drying circumstances.

Assuming symmetry, there are no temperature gradients or moisture concentration gradients in the slice's center, and as a result the following conditions hold [19];

$$\frac{\partial M}{\partial x} = 0 \ \& \ \frac{\partial T}{\partial x} = 0, \text{ at } x = 0, \quad (55)$$

$$\frac{\partial M}{\partial y} = 0 \ \& \ \frac{\partial T}{\partial y} = 0, \text{ at } y = 0, \quad (56)$$

$$\frac{\partial M}{\partial z} = 0 \ \& \ \frac{\partial T}{\partial z} = 0, \text{ at } z = 0. \quad (57)$$

At the outer surface, boundary conditions become[19]

$$\kappa \frac{\partial M}{\partial x} - \lambda D_0 \rho_s \frac{\partial T}{\partial x} = -h(T_{sur} - T_{air})$$

$$-D_0 \rho_s \frac{\partial M}{\partial x} = h_m(C_{sur} - C_{air}) \text{ at } x = L_x, \quad (58)$$

$$\kappa \frac{\partial M}{\partial y} - \lambda D_0 \rho_s \frac{\partial T}{\partial y} = -h(T_{sur} - T_{air})$$

$$-D_0 \rho_s \frac{\partial M}{\partial y} = h_m(C_{sur} - C_{air}) \text{ at } y = L_y, \quad (59)$$

$$\kappa \frac{\partial M}{\partial z} - \lambda D_0 \rho_s \frac{\partial T}{\partial z} = -h(T_{sur} - T_{air})$$

$$-D_0 \rho_s \frac{\partial M}{\partial z} = h_m(C_{sur} - C_{air}) \text{ at } z = L_z. \quad (60)$$

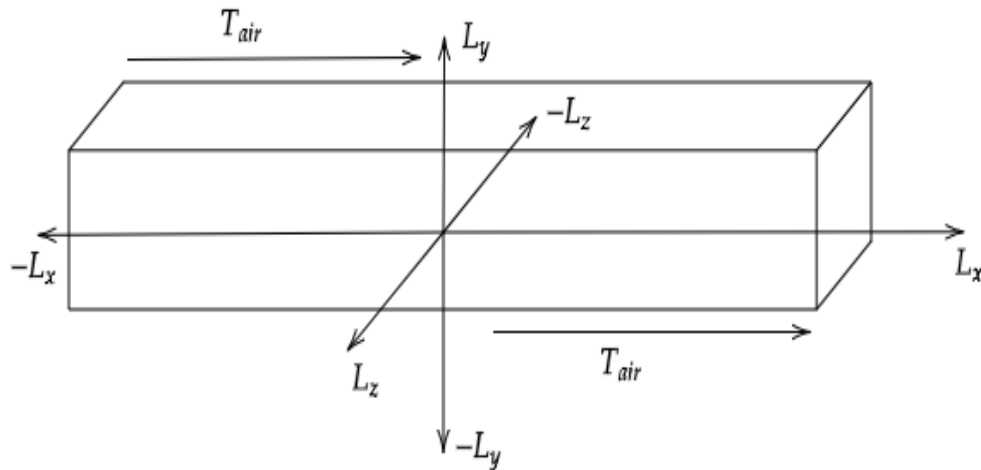


Figure 3: Schematic diagram of 3D model of drying fruit slice

Applying RDTM to (53) and (54), similar to 2D model, we can get the desired expressions for moisture content and temperature distribution in the fruit slice as below:

$$M(x, y, z, t) = M_0 [1 + \cos px \cdot \cos qy \cdot \cos rz \cdot e^{-D_0(p^2+q^2+r^2)t}], \quad (61)$$

$$T(x, y, z, t) = T_0 - T_1 \cos px \cdot \cos qy \cdot \cos rz \cdot e^{-\alpha_0(p^2+q^2+r^2)t}. \quad (62)$$

IV. RESULTS AND DISCUSSION

Mathematical models involving diffusion equations to describe moisture content and temperature distribution are solved for fruit slice considering 1D, 2D & 3D cases, using reduced differential transforms. For the analysis values of the parameters are taken as in Table II.

Table II: Values of parameters involved in the problem

Parameters and Symbols	Value	Unit
Diffusivity(D_0)	8×10^{-10}	$m \cdot s^{-1}$
Thickness(L_x)	5×10^{-3}	m
Width(L_y)	5×10^{-2}	m
Length(L_z)	5×10^{-1}	m
M_0	0.8	$\frac{kg.moist}{kg.sample}$
T_0	298	K
T_1	3	K
Thermal diffusivity(α_0)	1.31×10^{-7}	$m^2 \cdot s^{-1}$

A. Analysis for 1D Model

Solution in (21) and (22) of the 1D fruit drying model is obtained by solving two diffusion equations corresponding moisture (12) and temperature (13) in drying fruit slice.

Table III: Predicted moisture content at different time t for different layers in drying fruit slice

Time(sec)	$x = 0$	$x = \frac{L_x}{3}$	$x = \frac{L_x}{2}$	$x = \frac{2L_x}{3}$	$x = L_x$
$t = 0$	1.60	1.49	1.37	1.20	0.80
$t = 1000$	1.54	1.44	1.32	1.17	0.80
$t = 2000$	1.48	1.39	1.28	1.14	0.80
$t = 3000$	1.43	1.35	1.25	1.12	0.80
$t = 4000$	1.38	1.31	1.21	1.09	0.80
$t = 5000$	1.34	1.27	1.18	1.07	0.80
$t = 6000$	1.30	1.23	1.15	1.05	0.80
$t = 7000$	1.26	1.20	1.13	1.03	0.80
$t = 8000$	1.23	1.17	1.10	1.01	0.80

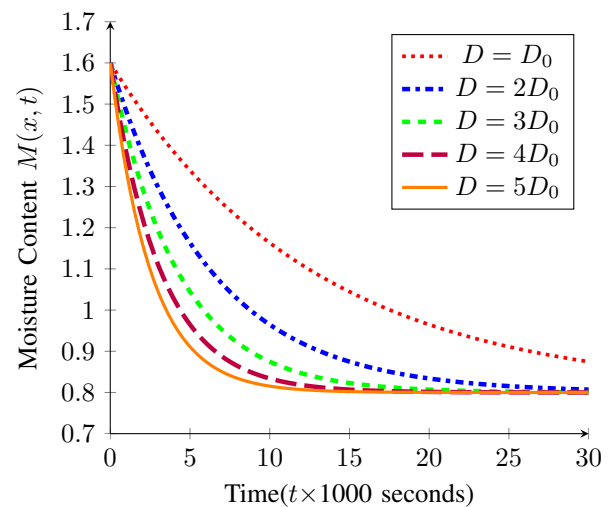


Figure 4: Effect of D_0 on moisture content inside the drying fruit slice

The table (III) shows the moisture of different layers of the fruit slice at different time intervals, predicted from this analytical solution. The graphical plot of the expression in (21) as figure (4) shows predicted moisture content in the center

of the slice over time for various diffusivity coefficients. From the figure, moisture content decreases significantly in the fruit slice with the increase in time t . This behavior of moisture content vs drying time from the analytical solution (21) is in close agreement with the findings shown in [22] from experimental results. The chosen values of diffusivity (D_0), slice thickness (L_x), and initial moisture level (M_0) have a significant impact on reducing moisture across all layers of the material. This effect is evident when examining the data in the table (III) and figure (4), where we can see that the moisture content drops significantly in all layers initially. The fruit is initially more saturated with water on the surface, and moisture is being removed at a faster rate. Moisture from within will diffuse onto the surface as the amount of surface moisture decreases. Diffusion takes place in the fruit from its interior to its exterior. For higher diffusivity coefficient D_0 values, the moisture content in the inner layers begins to significantly decrease as the drying process goes on.

Table IV: Predicted temperature at different time t for different layers inside drying fruit slice

Time(sec)	$x = 0$	$x = \frac{L_x}{3}$	$x = \frac{L_x}{2}$	$x = \frac{2L_x}{3}$	$x = L_x$
$t = 0$	295	295.4	295.879	296.5	298
$t = 50$	296.43	296.64	296.89	297.22	298
$t = 100$	297.17	297.29	297.42	297.59	298
$t = 150$	297.57	297.63	297.7	297.79	298
$t = 200$	297.77	297.80	297.84	297.89	298
$t = 250$	297.88	297.9	297.92	297.94	298
$t = 300$	297.94	297.95	297.96	297.97	298
$t = 350$	297.97	297.97	297.98	297.98	298
$t = 400$	297.98	297.99	297.99	297.99	298
$t = 450$	297.99	297.99	297.99	297.99	298

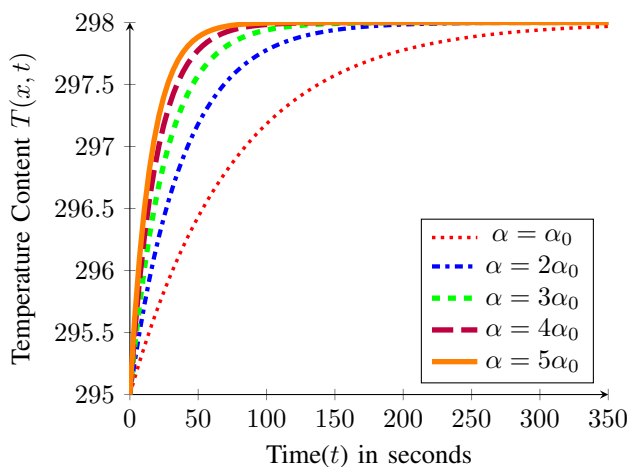


Figure 5: Effect of thermal diffusivity α_0 on temperature in the center of fruit slice at $x = 0$

Based on the figure (4), for the same time period the drying process accelerate with increased values of diffusivity coefficient and the lower the moisture content left inside the

fruit. This observation suggests that the diffusion process, which involves the movement of moisture within the fruit slice, can be significantly accelerated by adjusting the value of D_0 . In reality, several factors like temperature, moisture content, material composition, gradient concentration, etc. can affect the value of D_0 . Predicted from (22), table (IV) shows the temperature distribution within the fruit slice at the different interior layers, and figure (5) shows the temperature rise in the core of the slice. There is a temperature differential between the slice's surface and core. The surface temperature must initially rise and the heat transfer from the surface to the core must also rise in order to signal that the temperature inside the fruit has increased. There is a noticeable difference in the interior temperature between now and previously, and the notable rise suggests that the fruit slice's outer layer is getting hotter. This is in line with experimental findings by [11], which found that temperature distributions are higher at the outer surface and gradually decrease towards the interior portion of the moist object. The rate at which heat or temperature diffuses through a substance is measured by its thermal diffusivity. A high thermal diffusivity score indicates a quick change in temperature. It's interesting to see how quickly the fruit slice's temperature changes in this situation. It takes very little time to reach $298K$, which is a steady temperature. This stable temperature ($T_{sur} = 298K$) is in line with the ambient temperature of $298K$. In another way, the temperature of the fruit slice quickly changes to correspond with its environment. These findings indicate that the fruit's most exposed area tends to warm up more quickly. Therefore, the temperature at the fruit's core and surface will rise with a longer drying period.

B. Analysis for 2D model

The moisture content and temperature inside the 2-dimensional fruit slice is derived in (47) and (48) respectively. The figure (6) shows how moisture is distributed in the drying fruit slice and figure (7) shows the heat map for temperature inside the slice.

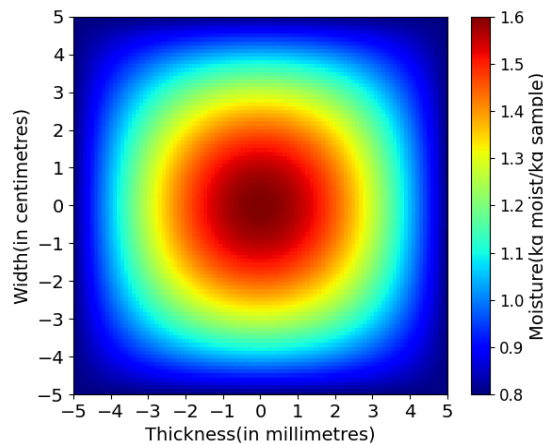


Figure 6: Heatmap for predicted moisture content inside the drying fruit slice(2D Model)

It's clear that the center of the fruit slice has the highest moisture, and it gradually decreases as we move away from the center. What's interesting is that in the 2D model, the moisture goes down faster compare to previous model. This

happens because the larger surface area in the 2D model allows moisture to escape more quickly into the surrounding environment. So, moisture decreases faster in the 2D model compared to the 1D model. This highlights the importance

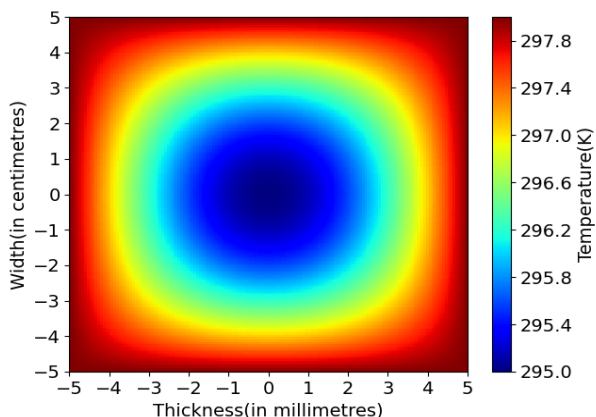


Figure 7: Heatmap for predicted temperature distribution inside the drying fruit slice (2D model)

of surface area and dimensions in understanding moisture behavior in the fruit slice. Investigating figure (7), it becomes evident that the temperature distribution within the 2D fruit slice exhibited a pronounced characteristic. The temperature profile reached its peak at the edges and gradually decreased as one moved towards the center. This intriguing behavior is attributed to the influence of surface area, which accelerates the rate of temperature rise. Prediction from the analytical solution given in figure (6) and (7) have same profile as in [19], the heat maps given in these figures show similar layered distribution of moisture content and temperature as discussed in [19] for 2D numerical study on drying fruit slice. In these plots the greater temperature and lower moisture content at the corners of the fruit slice are visible similar to the plots given in [19].

C. Analysis for 3D model

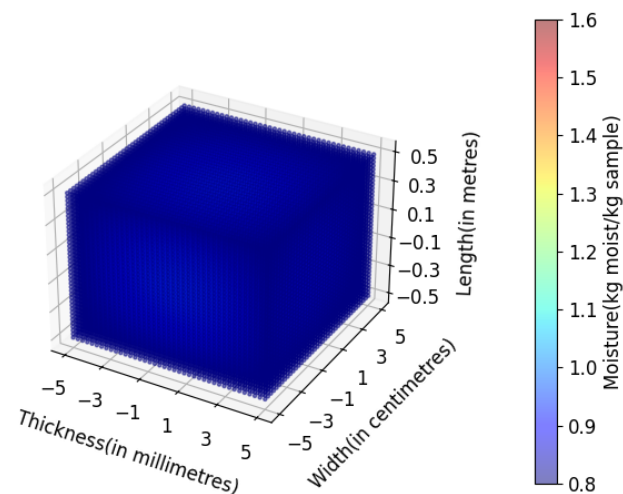


Figure 8: Moisture content inside the drying 3D fruit slice at initial point in time

The mathematical model for drying fruit slice is considered with three space variables in (53), (54) with extended initial moisture content (49) and initial temperature (50).

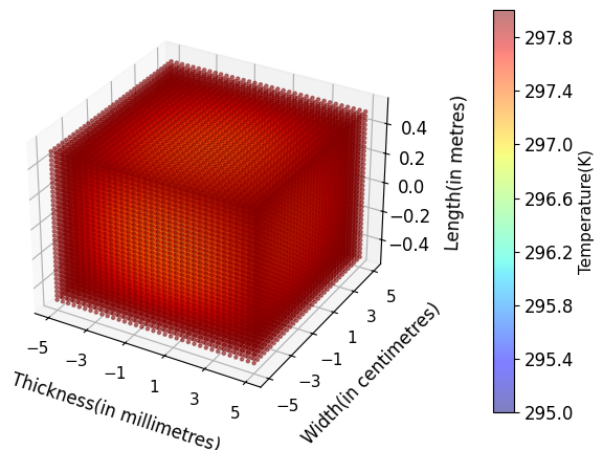


Figure 9: Temperature content in the drying 3D fruit slice at initial point in time

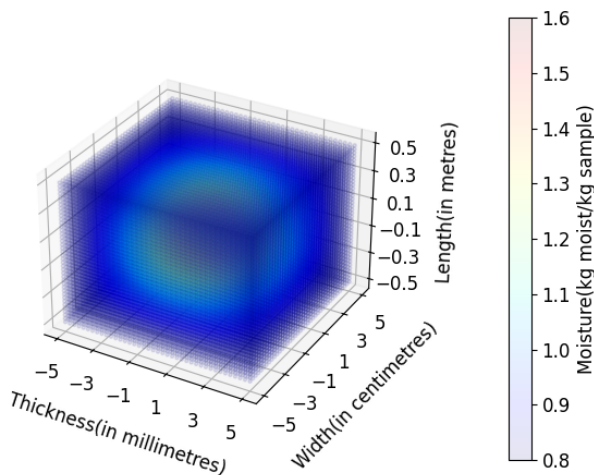


Figure 10: Transparent heat map for moisture content inside the drying 3D fruit slice at $t = 0$.

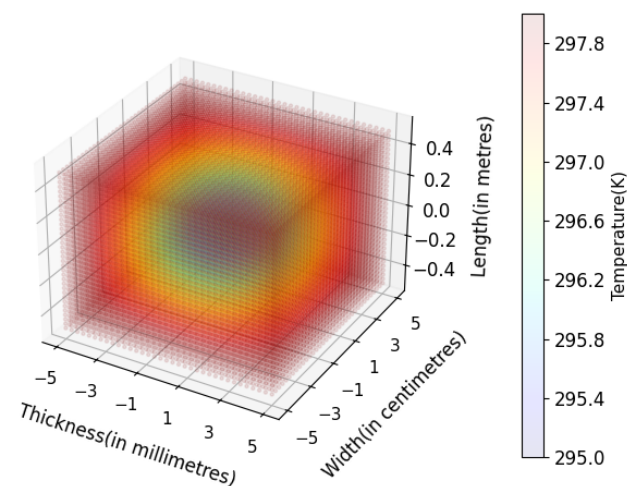


Figure 11: Transparent heat map for temperature content inside the drying 3D fruit slice at $t = 0$.

The analytical expressions derived in (61) and (62) give moisture content and temperature profile in this rectangular parallelepiped piece of fruit slice. The moisture content and temperature in the slice at $t = 0$ are shown in figure (8) and

figure (10) respectively. Figure (9) and (11) show the transparent heatmap through which the initial moisture content and initial temperature in the inner layers of the slice are seen. The figures (8) to (15) are 3D scatter plots generated by utilizing Matplotlib in Python. These visualizations help us to delve into the complexity of three space dimensions $x, y,$ and $z,$ representations are particularly insightful due to the addition of a nuanced fourth dimension time t conveyed through a color spectrum. This supplementary dimension serves the purpose of enlightening the moisture content at precise coordinates, enriching our comprehension of the dataset.

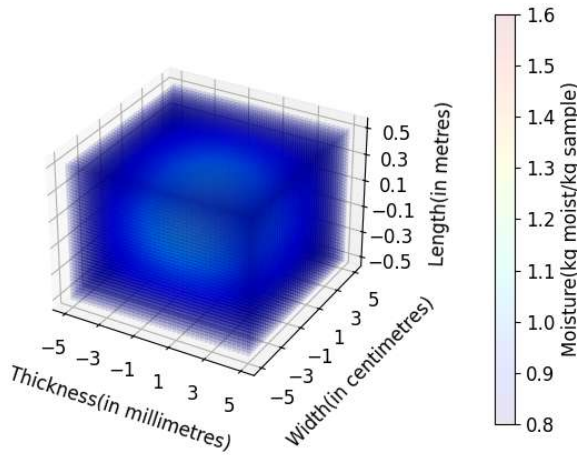


Figure 12: Transparent heat map for predicted moisture content distribution inside the drying 3D fruit slice at $t = 5000$.

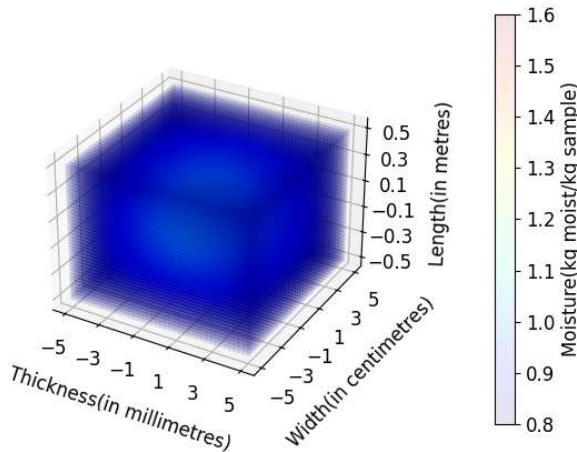


Figure 13: Transparent heat map for predicted moisture content distribution inside the drying 3D fruit slice at $t = 8000$.

Based on these analytical solutions (61) and (62) we have predicted the moisture content and temperature in the slice in figure (12), (13), (14) and (15). Figure (12) and (13) shows a transparent heatmap through which the moisture content in the inner part of the slice is visible at time $t = 5000$ sec and $t = 8000$ sec respectively. The transparent heatmaps in figures (14) and (15) portray temperature variations across different coordinates at time $t=50$ sec and $t=500$ sec respectively. Notably, the outer surface exhibits higher

temperatures than the inner surface, influenced by the heat exchange with the surrounding atmosphere.

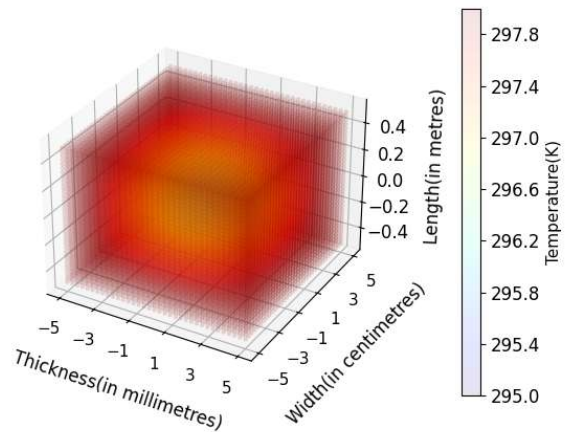


Figure 14: Transparent heat map for predicted temperature profile inside the drying 3D fruit slice at $t = 50$.

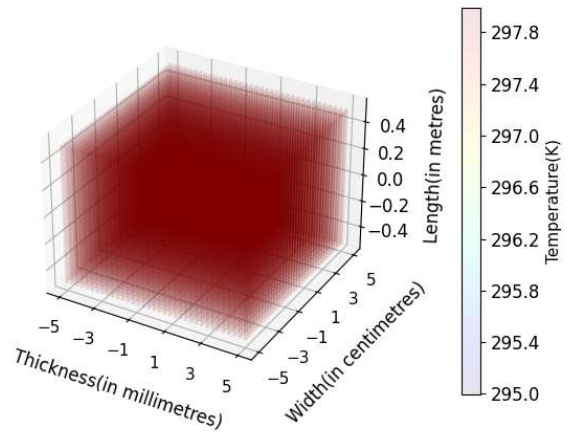


Figure 15: Transparent heat map for predicted temperature profile inside the drying 3D fruit slice at $t = 500$.

V. CONCLUSION

In order to investigate the behavior of moisture content temperature during the drying of fruit slice, 1D, 2D and 3D analytical model for removal of moisture content and temperature is developed. This model analytically represented the moisture removal and heat transmission during the drying process by using 1D case: very thin fruit slice, 2D case: slightly thick fruit slice and 3D case: rectangular parallelepiped shaped fruit slice to represent the drying fruit slice. Inside the fruit slice, the conduction mechanism is thought to happen as a heat transfer, whereas moisture removal is controlled by only liquid diffusion. The parameters thermal diffusivity and diffusivity coefficient are considered constant in all three models. Analytical solution is obtained by solving two diffusion equations corresponding to moisture and temperature in drying fruit slice using reduced differential transform method (RDTM), and it is analyzed by implementing the analytical model in Python together with the beginning conditions.

The results that we obtained in our study had critical insights into the moisture and temperature distribution in a fruit slice. One important observation is that a higher-dimension model yields the desired moisture and temperature faster than a lower-dimension model due to the effect of high surface area. A very interesting pattern is found in our models, moisture is highest at the center and lowest on the surface, whereas on the other hand, temperature is lowest at the center and highest on the surface. The surface of fruit slice that is exposed to the surrounding air warms up faster, reducing moisture content. The interconnection between thermal diffusivity (α_0) and moisture diffusivity (D_0) is responsible for such a pattern.

The suggested analytical model is able to offer information regarding moisture and temperature at all times in good agreement with the experimental and numerical studies performed earlier. In the analytical model we haven't considered the shrinkage effect in fruit slices, so it predicts temperature and moisture distribution throughout small span of time in the beginning of drying process. However, considering the shrinkage effect in fruit slices can make this model more realistic. Also, the inclusion of dependency of moisture diffusivity and thermal diffusivity on M and T respectively will bring us one more step closer to a realistic situation which can help us to understand the complexity of drying fruits.

REFERENCES

- [1] Yingjun Yu, Zhibin Ding, Xiao Chen, and Yaofeng Lu, "Review and development of the drying theory of porous medium," IOP Conference Series: *Earth Environment Science*, vol. 568, pp. 12-45, 2020.
- [2] N. Wang and J. G. Brennan, "A Mathematical Model of Simultaneous Heat and Moisture Transfer during Drying of Potato," *Journal of Food Engineering*, vol. 24, pp. 47-60, 1995.
- [3] N Shahari, H A Hasnan, A Y Hanan and N A H Noor Ishak, "Analysis of two-dimensional (2D) Fruit Drying Process through Heat and Mass Transfer Model," IOP Conf. Series: *Materials Science and Engineering*, vol. 477, pp. 12-24, 2019.
- [4] Lemuel M Diamante, Reiner Ihns, Geoffrey P Savage, and Leo Vanhanen, "A new mathematical model for thin layer drying of fruits," *International Journal of Food Science & Technology*, vol. 45(9), pp. 1956-1962, 2010.
- [5] İnci Tırnakçıoğlu and Dursun Pehlivan, "Modelling of thin layer drying kinetics of some fruits under open-air sun drying process," *Journal of Food Engineering*, vol. 65(3), pp. 413-425, 2004.
- [6] Shahpour Jahedi Rad, Mohammad Kaveh, Vali Rasooli Sharabiani, and Ebrahim Taghinezhad, "Fuzzy logic, artificial neural network and mathematical model for prediction of white mulberry drying kinetics," *Heat and Mass Transfer*, vol. 54, pp. 3361-3374, 2018.
- [7] J.A. Esfahani, H. Majdi and E. Barati, "Analytical two-dimensional analysis of the transport phenomena occurring during convective drying: Apple slices," *Journal of Food Engineering*, vol. 123, pp. 87-93, 2014.
- [8] Castro, A.M., Mayorga, E.Y. and Moreno, F.L., "Mathematical modelling of convective drying of fruits: A review," *Journal of Food Engineering*, 223, pp. 152-167, 2018.
- [9] S.M. Vahidhosseini, E. Barati, and J.A. Esfahani, "Green's function method (GFM) and mathematical solution for coupled equations of transport problem during convective drying," *Journal of Food Engineering*, Volume 187, pp. 24-36, 2016.
- [10] J. K. Zhou, "Differential Transform and its Applications for Electrical Circuits", Wuhan, China: Huarjung University Press, 1986.
- [11] Shadi al-Ahmad, Mustafa Mamat, and Rami al-Ahmad, "Finding Differential Transform Using Difference Equations," *IAENG International Journal of Applied Mathematics*, vol. 50, no. 1, pp. 127-132, 2020.
- [12] F.Ayaz, "Solutions of the system of differential equations by differential transform method," *Applied Mathematics and Computation*, vol. 147, no.2, pp. 547-567, 2004.
- [13] Y.Huang, "Explicit multi-soliton solutions for the KdV equation by Darboux transformation," *IAENG International Journal of Applied Mathematics*, vol.43, no.3, pp. 135-137, 2013
- [14] H.Song, M.Yi, J.Huang and Y.Pan, "Bernstein polynomials method for a class of generalized variable order fractional differential equations," *IAENG International Journal of Applied Mathematics*, vol. 46, no.4, pp. 437-444, 2016.
- [15] Adio, A., "Application Of Reduced Differential Transformation Method for Solving System of Nonlinear Partial Differential Equations (Pdes)," *International Journal of Applied Mathematics & Statistical Sciences (Ijamss)*, 5, pp. 63-70, 2016.
- [16] Yildiray Keskin and Galip Oturanc, "The reduced differential transform method: a new approach to fractional partial differential equations," *Nonlinear Sci. Lett. A*, vol. 1(2), pp. 207-217, 2010.
- [17] Yildiray Keskin and Galip Oturanc, "Reduced differential transform method for generalized kdv equations," *Mathematical and Computational Applications*, vol. 15(3), pp. 382-393, 2010.
- [18] Yildiray Keskin, Sema Servi, and Galip Oturanc, "Reduced differential transform method for solving Klein Gordon equations," *Lecture Notes in Engineering and Computer Science: Proceeding of the World Congress on Engineering 2011*, 6-8 July, 2011, London, U.K., pp123-127.
- [19] Nor Azni Shahari, "Mathematical modeling of drying Food products: application to tropical fruits, Ph.D. thesis," *University of Nottingham*, 2018.
- [20] W.A.M. McMinn, T.R.A. Magee, "Principles, methods and applications of the convective drying of Food stuffs," *Food and Bioprocess Processing*, vol.77, pp. 175-193, 1999.
- [21] Moosavi Noori, S.R. and Taghizadeh, N. "Study of convergence of reduced differential transform method for different classes of differential equations," *International Journal of Differential Equations*, pp. 1-16, 2021.
- [22] Mohan, V.C. and Talukdar, P. "Three-dimensional numerical modeling of simultaneous heat and moisture transfer in a moist object subjected to convective drying," *International Journal of Heat and Mass Transfer*, 53(21-22), pp. 4638-4650, 2010.